A New Test Facility for Advanced Testing of Variable Inlet Guide Vanes

Roman G. Frank[1*], *Christian* Wacker[2], and *Reinhard* Niehuis[1]

[1]Bundeswehr University Munich, Institute of Jet Propulsion, 85577 Neubiberg, Germany
[2]MAN Energy Solutions SE, ECC Integrally Geared Compressors, 13507 Berlin, Germany

Abstract. Various experimental and numerical studies of advanced blade configurations for variable inlet guide vanes (VIGVs) were conducted during the past years. Nevertheless, experimental loss characterizations of VIGV blade designs vastly focused on the primary profile losses. Secondary flow losses as they occur in a real engine application were often neglected. For this reason, a new wind tunnel facility was erected and commissioned at the Bundeswehr University Munich to enable extensive investigations of application-oriented annular VIGV configurations at typical low subsonic Mach numbers. Five-hole probe field traverses are established by a probe traversing unit in the in- and outflow region of the VIGV. The requirements for a further extension of the applicable measuring techniques by optical methods is moreover provided. Thus, not only profile losses caused by the blades, but also secondary flow losses generated by blade-wall flow interactions and the open blade tips can be resolved in detail.

1 Introduction

Integrally geared compressors with a multi-shaft centrifugal design as illustrated in Figure 1 are commonly used as the supply of manifold gases in the energy intensive petrol and chemical industry as well as air separation units, see Beaty et al. [1]. Two to ten centrifugal compressor stages are driven by a single common bull gear via up to five shafts. Depending on the amount of stages and the compressor scale, discharge pressures and maximum suction flow rates reach 250 bar and 150 m^3/s.

Aiming for a flexible compressor operation, an efficient partial load operation is indispensable. Generally, two options are therefore considered;

a) the variation of the pinion shaft speed
b) and the pre-swirl control in potential combination with a variable vaned diffuser as described by Simon et al. [2].

As the shaft speed is usually linked to the mains frequency by the powering synchronous motor, only the pre-swirl control by a VIGV remains feasible in most applications.

Naturally, the low loss operating range of VIGVs and, thus, of the total integrally geared compressor is limited by the efficient flow deflection range of the VIGV blades. In order to extend the operation limits, common blade designs were reconsidered. Stark & Böhle [3] and Mohseni et al. [4] tested a variety of airfoil concepts with respect to an increase of the efficient deflection range. Their most promising approach, the split vane, was further developed and evaluated by Händel et al. [5]. These measurements, however, include only profile losses. Secondary flow effects were not considered in these linear cascade measurements; neither in the mentioned experiments nor within further known experimental investigations.

Due to the superimposition of profile and secondary flow losses in annular VIGVs, it has to be expected that the predicted improvements of the efficient VIGV deflection range based on linear cascade measurements will not fully apply to the application in service. In order to take the loss mechanisms induced by the three-dimensional design into account, a new wind tunnel for annular cascades was set up and commissioned at the facilities of the Institute of Jet Propulsion at the Bundeswehr University Munich.

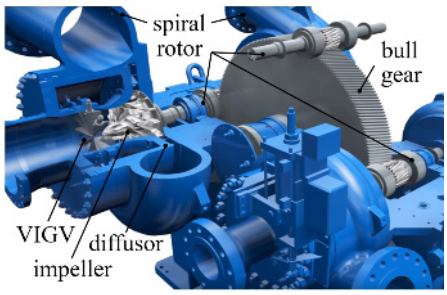

Fig. 1. Cross section of an integrally geared compressor

2 Experimental Setup

2.1 Metrological Objective

The primary goal of the VIGV wind tunnel is the metrological analysis of the flow performance of varied VIGV configurations at various stagger angles and operating points. The flow performance is determined by highly resolved field measurements in the wake of the VIGV specimen. Especially two major parameters determine

* Corresponding author: roman.frank@unibw.de

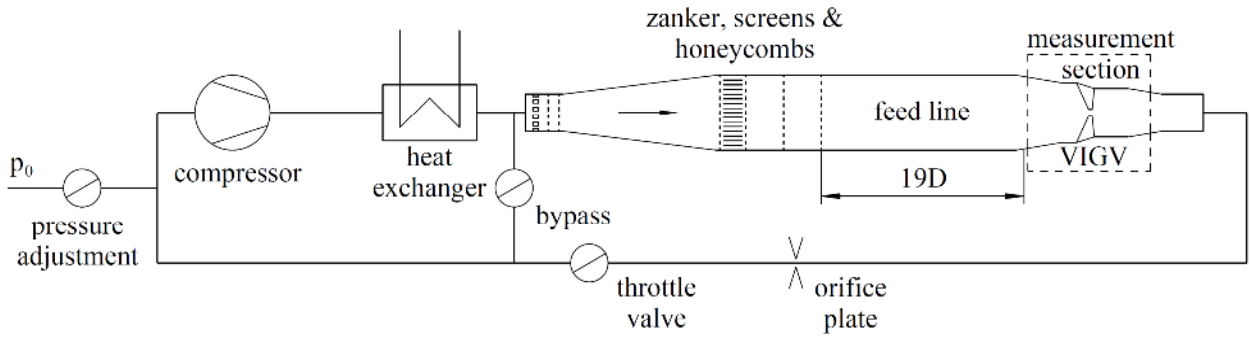

Fig. 2. General layout of the VIGV test facility

the quality of the VIGV cascade performance: the flow deflection $\Delta\beta$ and the associated total pressure loss coefficient ζ. The latter is described as the total pressure loss p_{t1}- p_{t2} between the VIGV in- and outlet relative to the mean dynamic pressure q_1 at the inlet

$$\zeta = \frac{p_{t1} - p_{t2}}{q_1}. \tag{1}$$

As a distinct velocity profile is expected at the inlet of the VIGV, q_1 is based on an integral definition of the dynamic pressure across the inlet. It is therefore deducted by the static pressure p_1 at the VIGV inlet and the mean inlet Mach number Ma_1:

$$q_1 = p_1 \left(\left[1 + \frac{\gamma - 1}{2} Ma_1^2 \right]^{\frac{\gamma}{\gamma - 1}} - 1 \right) \tag{2}$$

In contrast, the total pressure loss induced by the vane $p_{t1} - p_{t2}$ is based on local measurements in the inflow region and the wake of the VIGV.

2.2 General Wind Tunnel Design

The VIGV features a closed loop wind tunnel design with the general opportunity to adjust the operating pressure. An outline of the general layout is found in Figure 2. The airflow of the wind tunnel is provided by a MAN GHH Skül 408 screw compressor with a volumetric flow rate of approximately 5.4 m^3/s and a maximum pressure ratio of 3.2. A subsequent heat exchanger ensures steady temperature levels down to at least 300K.

Subsequently, the total air flow through the measurement section can be reduced by a bypass. The remaining mass flow passes a variety of flow conditioners, the feed line and, finally, the measurement section including the VIGV specimen illustrated in Figure 3. Downstream the measurement section, the mass flow rate is determined by orifice plates. The pressure level in the measurement section can furthermore be adjusted by an integrated throttle valve.

2.3 Operating Point

According to common practice in compressor technology, the definition of the operating point or the Mach and Reynolds number (Ma & Re), is related to the VIGV inflow conditions. These can be fully specified by the VIGV inlet diameter D_1, the static pressure at the inlet p_1, the temperature T and the mass flow rate $\dot{m}$. Due to a distinct velocity profile at the VIGV inlet, the integral defintion of the operating point based on the mass flow rate $\dot{m}$ is chosen. The boundary layer of the incoming flow is therefore taken into account.

During the wind tunnel operation at atmospheric compressor inlet conditions, application-oriented flow conditions of up to Ma = 0.125 and Re = 1.16×10^6 can be achieved reproducibly.

$$Ma = \frac{4}{\pi} \frac{\dot{m}}{p_1 D_1^2} \sqrt{\frac{RT}{\gamma}} \tag{3}$$

$$Re_D = \frac{4}{\pi} \frac{\dot{m}}{\mu D_1} \tag{4}$$

2.4 Control Unit

Consistent Ma and Re numbers are maintained by the control unit utilizing the three installed valves. The bypass valve mainly controls the mass flow rate through the measurement section, whereas the pressure adjustment valve and the throttle valve primarily affect the general static pressure level in the measurement section. An increase of the pressure in the measurement section is obtained by the throttle valve within the ranges of the compressor. Absolute VIGV inlet pressure levels of 1.4 to 2.4 bar are thus feasible. In order to reduce the pressure level for a widened range of Ma and Re numbers, an additional vacuum pump is applicable. Alongside the already addressed bypass, a mass flow reduction by maximum 45% can be accomplished by a decrease of the rotational speed of the compressor.

Due to the ability to control the volumetric flow rate as well as the static pressure in the measurement section, an independent variation of the Mach and Reynolds number is possible within the limits of the available static pressure levels and the possible mass flow rates. Furthermore, the fully automated control of the three valves allows a reliable setting of the operating point throughout the operating time. Mach and Reynolds number variations during the measurements can thereby be limited to ±0.2%.

2.5 Feed Line

The feed line consists of a diffusor, a long straight pipe and a conical nozzle with a moderate area ratio between

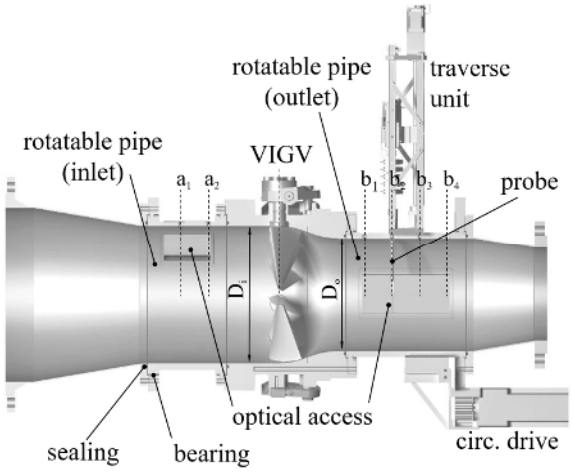

Fig. 3. Layout of the measurement section

outlet and inlet of 63%. In order to avoid excessive pressure losses due to separation, the diffusor in the feed line is designed with a constant opening angle of 12° according to Pope and Harper [6]. The suggestion represents a compromise between the ideal opening angle of 8° in regard to pressure losses as described by Truckenbrodt [7] and a reasonable diffusor length.

Besides the common approach to provide room for flow conditioners at decelerated flow velocities, the general design of the feed line serves the replication of the inflow velocity profile to integrally geared compressors. Therefore, the feed line features an unhindered straight DN400 pipe segment of the length of 19 times the pipe diameter and a subsequent, conically shaped nozzle upstream the measurement section. A geometric similarity to the setup of the industrial application is thus maintained.

2.6 Applicable VIGVs

For the commissioning of the wind tunnel, a VIGV commonly used in industry as illustrated in Figure 4 was utilized. The VIGV configuration is kindly provided by MAN Energy Solutions SE and consists of eleven, symmetric blades arranged along the circumference. All blades are turned as a group by an external linkage. Based on the requirement to ensure arbitrary stagger angles down to β_S = 90°, resp. the closing of the VIGV cross section, the blades are shaped trapezoidal. Clearance between the casing and the blade root is avoided by a spherically constructed duct in the VIGV as shown in Figure 3. Significant losses can thus be avoided, see Coppinger and Swain [8].

The VIGV test facility is, however, not limited to this particular VIGV. Based on the variable design of the interfacing flange connections, a variety of VIGVs with modifications like varied profile concepts, twisted blade geometries or a hub, resp. centerpiece, can be installed and investigated by minor effort. This permits the comparison of different design concepts among each other as well as the identification of a particularly favourable configuration.

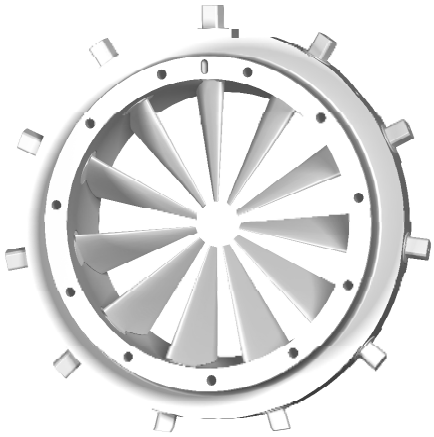

Fig. 4. State of the art VIGV, MAN Energy Solutions

2.7 Traverse Unit

Generally, two options to investigate the flow characteristics of VIGVs are provided at the VIGV test facility; windows for optical measuring procedures and the traverse unit for the application of probe measurement technology. The latter features the fully automated, local positioning of arbitrary, cranked probes in high resolution within the relevant cross sections. It is designed in order to provide probe access both to the inflow and the outflow region of the VIGV. In total, six discrete cross sections can be accessed as outlined in Figure 3. The first two cross sections a_1 and a_2 are located 0.71 and 0.51 times the VIGV inlet diameter D_i upstream the plane of the rotational axis of the VIGV blades. The remaining four probe supply bores are located at b_1 to b_4 0.61, 0.81, 1.01 and 1.21 times D_i downstream the same reference plane.

The circumferential movement is accomplished by two rotatable pipe segments at the inflow and the outflow of the VIGV shown in Figure 3. Each pipe segment is guided by two thin section roller bearings. This space-saving design enables an axial probe position as close to the VIGV as possible. In order to avoid leakage along the thin section bearing, a sealing is inevitable. Due to the considerable large circumference of the pipe segments, the specific friction forces of the sealing, however, need to be kept small to ensure a motion in control despite the torque limitations of the driving unit. For this reason, PTFE lip seals are implemented between the rotating end plate and the subsequent, rigid flange, see Figure 5. This, in combination with a 40 Nm stepper motor

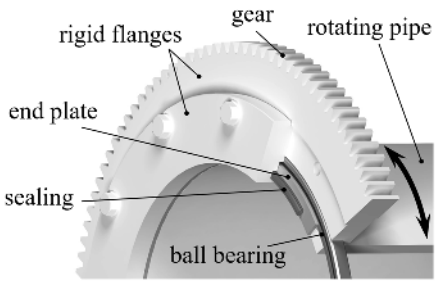

Fig. 5. Bearing and sealing concept of the two rotating pipe segments

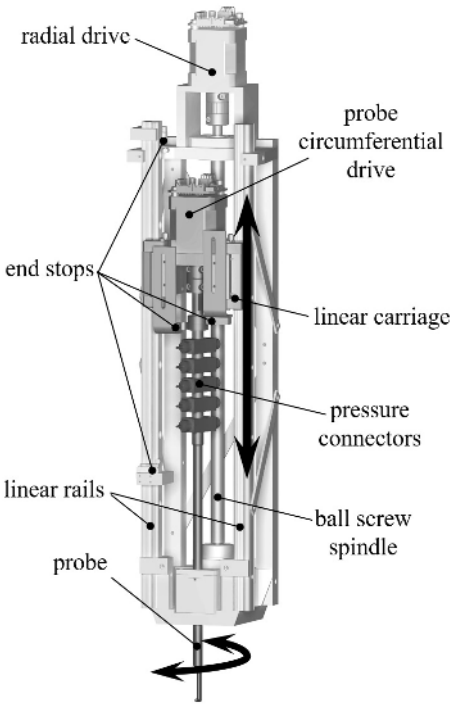

Fig. 6. Radial and probe circumferential traverse

and a 5.5-fold gear reduction between the rigid flange and the motor mounted on the rotating pipe segment, permits a smooth and reliable control of the circumferential traverse. In order to minimize the backlash of the transmission, the gear features an involute tooth design. The final, total uncertainty of the circumferential traverse position adds up to ±0.2°. If the traverse is moved into one direction only, the positioning uncertainty is even reduced down to a maximum of ±0.1°.

The radial positioning of the probe, in contrast, is carried out along a linear guide rail. Both probe and carriage are driven by a ball screw spindle and a 20 Nm torque motor illustrated in Figure 6. This design enables an accurate positioning along the radial axis. The uncertainties based on the clearance of the gear or thermal expansion are considered negligible small compared to those arising from the calibration process. The calibration accuracy is estimated to be lower than ±0.1mm.

Due to anticipated high gradients of the circumferential flow deflection, especially along the radius downstream the blade tip region, a third stepper motor is implemented to automatically pivot the probe along the shaft axis into the calibration range, see Figure 6. Measurements off the calibration range can thus be avoided.

The entire traverse unit is designed without a dedicated decoupled feedback system consisting of rotary and linear encoders. Instead, the advantage of stepper motors in regard to their position accuracy is exploit.

2.8 Pneumatic measurement

In order to measure the crucial flow parameters $\Delta\beta$ and ζ, the cranked five-hole probe shown in Figure 7 with a short probe head and a 3 mm head diameter was utilized for the first wake traverse measurements on the VIGV wind tunnel. Generally, five-hole probes allow a firm local detection of the total pressure alongside the flow velocity and its spatial components [9]. Based on the short-cranked probe head, the probe can be pulled into the radial and circumferential traverse body (Figure 6), whereby a gentle and fast mounting is ensured. The calibration of the probe was executed in an angular range of ±24° and from Ma numbers of 0.05 to 0.6. The differential pressures at the probe as well as the remaining pressure taps at the measuring section are recorded by a Netscanner 98RK with the full range of available pressure transducers from 10''WC (0.36 PSI) to 15 PSI. Thus, customized pressure transducers in accordance with the wind tunnel settings can be used for the five-hole probe measurement.

In the particular case of five-hole probes, the coarse alignment into the flow can easily be accomplished by balancing the differential pressure between the opposite pressures taps.

2.9 Optical Access

To avoid limitations of the test stand to probe measurement technologies only, the fundamental requirements for optical measurement techniques were considered during the setup of the VIGV wind tunnel facility. Therefore, optical access to the flow is available by 9 mm thick, curved borosilicate glass panes at the in- and outflow region of the guide vane. Two windows are located in the inflow region; the remaining three windows in the outflow section. Probe measurement techniques, like five-hole probes or hot wire anemometry, can hence be complemented by optical methods without the spatial restrictions of the probe procedures. Particle image velocimetry (PIV), as described by Westerweel [10], for instance, supplements the probe measurements in the wake and the secondary flow regions, whereas the pressure sensitive paint technique (PSP) provides the opportunity to gain the pressure distribution on the entire blade surface as described by Liu and Sullivan [11]. Both measurement techniques are well established at the Institute of Jet Propulsion, see Bitter and Niehuis [12] and Bitter et al. [13].

Fig. 7. Utilized cranked five-hole probe with a 3mm probe head diameter

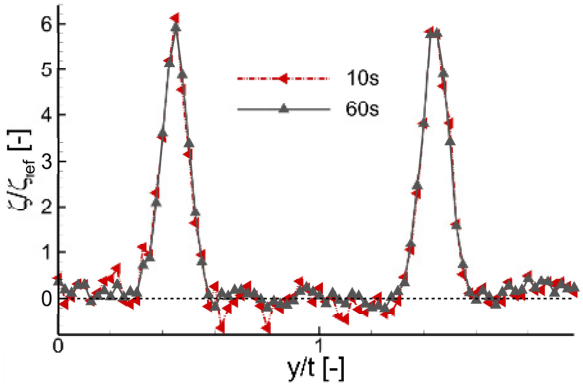

Fig. 8. Influence of the measurement time with respect to the temporal mean average (3 screens, $\boldsymbol{\beta_S}$ = 90°)

2.10 Flow Conditioning

Due to infrastructural reasons, the air feed towards the measurement section is realized via a 90° bend of a T-section pipe which causes significant unsteadiness of the local total pressure level. In a highly unsteady flow, it is particularly challenging to measure reliable temporal mean values as the standard deviation of a mean $\bar{\sigma}$ decreases only linearly by the quadratic increase of the samples n, resp. the measurement time, see Everitt and Skrondal [14]:

$$\bar{\sigma} = \frac{\sigma}{\sqrt{n}} \qquad (5)$$

This effect is illustrated by a representative wake traverse at β_S = 90° in Figure 8. In total, only three screens downstream of the diffuser were implemented at this stage. The unsteadiness of the flow in the measurement section was therefore only slightly dampened. Accordingly, significant fluctuations and outliers characterize the measurements based on periods of 10s. Nevertheless, extended measurement times of 60s result only in a comparable small decrease of the noise although the excessive increase of measurement time which is hardly practicable for highly resolved wake field measurements.

In order to reduce the flow unsteadiness in the measurement section and to obtain more precise measurements at a justifiable recording time, the amount of flow conditioners was considerably increased as recommended by Scheiman [15]. The final configuration of the flow conditioners features four screens and one set of honeycombs downstream as well as two screens and one Zanker module described by Laws and Ouazzane [16], upstream of the diffusor as shown in Figure 9. As

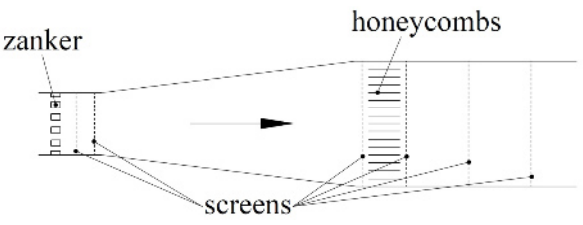

Fig. 9. Arrangement of the flow conditioners

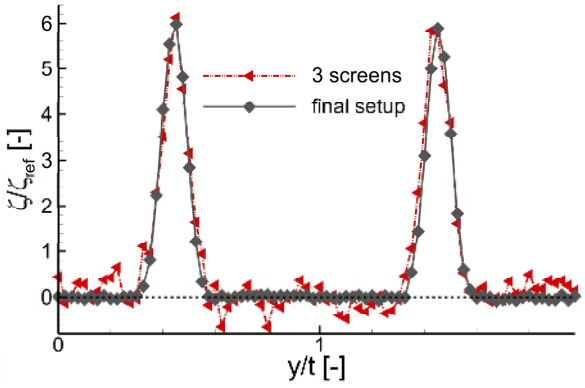

Fig. 10. Reduction of temporal fluctuations by flow conditioners (t = 10s, $\boldsymbol{\beta_S}$ = 90°)

a result, the flow unsteadiness was reduced to an acceptable level of $\bar{\sigma}_\zeta \approx 0.05\%$. A comparison of the exemplary wake traverse recorded at the previous setup with the three screens and the final configuration is depicted in Figure 10. Additional intermediate measurements underlined the particular positive effect of the flow conditioners upstream the diffusor. It is anticipated that diffusor instabilities were thus largely avoided. The positive effect of screens upstream of the diffusor in order to avoid diffusor instabilities was also demonstrated by Fadilah and Erawan [17] and Hasselmann et al. [18].

Besides the homogenization and smoothening influence, the resilience of the 25 mm thick Zanker module has to be highlighted in particular. As the unconditioned flow causes significant alternating stresses on the initial flow conditioners, the robustness of the first flow conditioner in particular had to be ensured in this application to avoid a fatigue failure of the screens.

3 Inflow conditions and correlation

Measurements upstream the VIGV at the axial position a_1 and the operating point Ma = 0.125 and Re = 1.16×10^6 revealed a distinct total pressure distribution shown in Figure 11. Whereas the circumferential variations remain low, a pronounced profile of ζ is observed along the radius. Nevertheless, the profile is still considerably flat compared to the shape of a fully developed total pressure distribution in a smooth pipe, see Figure 12. This is consistent due to a certain surface roughness,

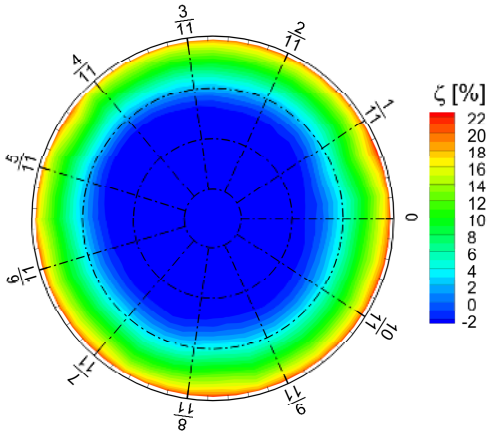

Fig. 11. Inflow conditions upstream the VIGV

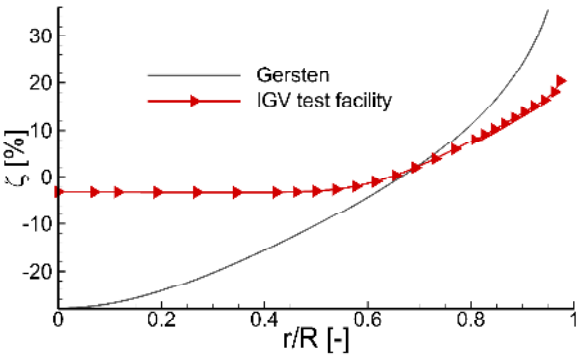

Fig. 12. Mean radial inflow characteristic of the VIGV test facility versus the characteristic of a smooth pipe according to Gersten [19]

the limited feed length and the flow acceleration in the nozzle.

As the total pressure loss coefficient ζ refers to the total pressure p_{t1} measured by a pitot probe at an arbitrary, fixed position 1.5m upstream the cascade, ζ appears as a distinct loss and gain distribution at the inlet plane. It is self-evident that this inlet constraint, if not considered, will cause a systematic error in the loss characterization of the actual VIGV.

In order to prevent this bias error, $p_{t1} - p_{t2}$ is ideally recorded simultaneously along one stream line. For practical reasons, the simultaneous measurement of the correlating values is not feasible by intrusive probe technology. Separate measurements of ζ up- and downstream the VIGV (ζ^i and ζ^o) are therefore required. Provided that the p_{t1} reference remains the same during both measurements a correlated value ζ^c can be conducted as follows:

$$\zeta^c = \frac{\zeta^o q_1^o - \zeta^i q_1^i}{q_1^o} \tag{6}$$

Due to the automated control system, only minor operating point variations between the two measurements at the in- and outlet plane can be assumed, i.e. the recorded pressures at the pitot probe $p_{t1,pit}^i$ and $p_{t1,pit}^o$ remain approximately equal. The total pressure drop along the VIGV can therefore be stated as a function of independent measurements:

$$\zeta^c \approx \frac{p_{t1,fhp}^i - p_{t2,fhp}^o}{q_1^o} \tag{7}$$

In order to identify the position of the matching ζ^i and ζ^o, solely the radial displacement of the streamlines is considered at this stage. The displacement is caused by the reduction of the casing diameter along the VIGV. Based on the assumption of a constant mass flow density, the radial position can be correlated by the non-dimensional radius $\bar{r} = r/R$.

4 Exemplary Results

Although the general objective of this paper focuses on the new VIGV test facility and the accompanying data

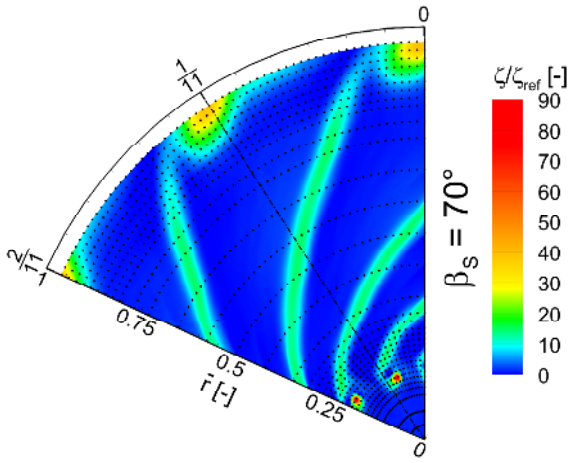

Fig. 13. Correlated total pressure loss coefficient at βs = 70°

processing routine, the ability to measure highly resolved flow fields shall be demonstrated by an exemplary measurement at a stagger angle of β_S = 70°. Due to an assumed circumferential symmetry of the flow characteristics and simple economic reasons, a reduction of the investigated cross section down to two of the eleven pitches was undertaken. Nevertheless, 33 circumferential traverses and in total 1108 single measurement points were recorded for the loss characterization of this particular setup.

Without going into an in-depth analysis of the flow field, the exemplary field at β_S = 70° as depicted in Figure 13 still emphasises the full three-dimensional flow effects occuring at annular VIGV cascades. Generally, the loss characteristic shown in Figure 13 can be split into four specific regions:

a) The core region of undisturbed flow downstream the blow hole at $\bar{r} < 0.2$,
b) the region of the blade tip vortex at $\bar{r} \approx 0.2$ caused by the free ending of the blade,
c) the region mainly dominated by primary blade profile losses between $0.25 \leq \bar{r} \leq 0.85$
d) and the region dominated by wall interactions of the flow at $\bar{r} > 0.85$

This exemplary measurement already substantiates the establishment of a test facility in order to resolve both profile and secondary losses of an actual VIGV cascade. As intended, not only the blade losses, which were already investigated in linear cascade measurement by Händel et al. [20], but also losses induced by wall or blade tip interactions can be fully resolved and investigated.

5 Summary & Outlook

The presented test facility at the Bundeswehr University Munich offers the opportunity to investigate the aerodynamic performance of state-of-the-art, annular VIGV cascades at application oriented Ma and Re numbers. Based on a flexible design of the facility, various VIGV blade concepts can be tested without a significant reconstruction of the measurement section. In contrast to previous investigations of advanced VIGV blade concepts

on linear cascades, not only profile losses but also secondary flow losses induced by the annular cascade design are reproduced at the VIGV test facility.

Initial measurements at the VIGV test facility were conducted by five-hole probe technology. Smooth flow conditions are ensured by a significant amount of flow conditioners. Thus, the recording of highly resolved flow fields becomes feasible within justifiable measurement times. Accordingly, an application-oriented qualification and understanding of the overall losses of annular VIGVs is now possible. This in combination with the flexible design of the measurement section helps to identify more progressive VIGV configurations with an increased low-loss-working range.

In addition to the currently installed pneumatic probe technology, the application of optical measurement techniques, like PIV and PSP, is intended for future research activities. PIV and PSP either supplement already available probe technology in the wake or even extend the available measurement range with respect to the flow mechanisms occurring along the blade surface.

Acknowledgments

The authors gratefully acknowledge the financial support of the Kopernikus project SynErgie by the German Federal Ministry of Education and Research (BMBF) and the project supervision by the project management organization Projektträger Jülich (PtJ).

Nomenclature

Symbols

D	[m]	Diameter
$\dot{m}$	[kg/s]	Mass flow
n	[-]	Samples
Ma	[-]	Mach number
μ	[Pa·s]	Dynamic viscosity
p	[Pa]	Pressure
q	[Pa]	Dynamic pressure
R	[J·kg^{-1}·K^{-1}]	Specific gas constant
Re	[-]	Reynolds number
T	[K]	Temperature
σ	[-]	Standard deviation
β	[°]	Angle
γ	[-]	Heat capacity ratio
ζ	[-]	Total pressure loss coefficient

Sub-/Superscripts

c	Correlated
fhp	Five-hole probe
i / o	Probe at VIGV in- / outlet
pit	Pitot probe
s	Stagger
t	Total
1 / 2	Position up- / downstream the VIGV

Abbreviations

PIV	Particle Image Velocimetry
PSP	Pressure Sensitive Paint
VIGV	Variable Inlet Guide Vane

References

1. P. J. Beaty, K. Eisele, T. D. Maceyka and C. Schwarz, *Integrally Geared API 617 Process Gas Compressors*, in Proceedings of the 29th Turbomachinery Symposium, Texas A&M University, USA (2000)
2. H. Simon, T. Wallmann and T. Mönk, *Improvements in Performance Characteristics of Single-Stage and Multistage Centrifugal Compressors by Simultaneous Adjustments of Inlet Guide Vanes and Diffusor Vanes*, in ASME J. Turbomach., **109**, 1 (1987)
3. U. Stark and M. Böhle, *Theoretische und experimenteile Untersuchungen an ungestaffelten Gittern aus Profilen mit mechanischen Klappen*, in Forschung im Ingenieurwesen, **56**, 6 (1990).
4. A. Mohseni, E. Goldhahn, R. A. Van den Braembussche and J. R. Seume, *Novel IGV Designs For Cetrifugal Compressors And Their Interaction With The Impellor*, J. Turbomach., **134**, 2, (2012)
5. D. Händel, R. Niehuis and J. Klausmann, *Aerdoynamic Investigations of an Advanced VIGV Design of Adjustable Geometry for Very High Flow Turning*, in Proceedings of ASME Turbo Expo, GT2015-42166, Montreal, Canada (2015)
6. A. Pope and J. Harper, Low-Speed Wind Tunnel Testing, New York: Wiley & Sons (1966)
7. E. Truckenbrodt, Lehrbuch der angewandten Fluidmechanik, Berlin: Springer-Verlag (1988)
8. M. Coppinger and E. Swain, *Perfomance Prediction of an Industrial Centrifugal Compressor Inlet Guide Vane System*, in Journal of Power and Energy, **214**, 2 (2000)
9. D. Bryer and R. Pankhurst, Pressure-Probe Mehtods for Determining Wind Speed and Flow Direction, London: Her Majesty's Stationery Office (1971).
10. J. Westerweel, *Fundamentals of Digital Particle Image Velocimetry*," in Meas. Sci. Technol., **8** (1997)
11. T. Liu and J. P. Sullivan, Pressure and Temperature Sensitive Paints, Berlin: Springer (2005)
12. M. Bitter and R. Niehuis, *Effects of Periodic Inflow Turbulence on the Statistics in the Wake of a Linear LPT Cascade at Jet-Engine relevant Test Conditions*, in 13th International Symposium on Particle Image Velocimetry, Munich, Germany (2019)
13. M. Bitter, S. Stotz and R. Niehuis, *On High-Resolution Pressure Amplitude and Phase Measurements Comparing Fast-Response Pressure Transducers and Unsteady Pressure-Sensitive Paint*," in J. Turbomach., **143**, 3, (2021)
14. B. Everitt and A. Skrondal, The Cambridge Dictionary of Statistics, Cambridge: Cambridge University Press (2010)

15. J. Scheiman, *Comparison of Experimental and Theoretical Turbulence Reduction Characteristics for Screens, Honeycomb and Honeycomb-Screen Combinations*," in J. Aircraft, **18**, 8, (1981)
16. E. M. Laws and A. K. Ouazzane, *A Further Study into the Effect of Length on the Zanker Flow Conditioner*, in Flow Meas: Instrum., **6**, 3 (1995)
17. P. A. Fadilah and D. F. Erawan, *Effect of Applying Screen and Honeycomb to the Flow Characteristic in Wind Tunnel Based on CFD Sumulation*, in J. Phys.: Conf. Ser., **1130** (2018)
18. K. Hasselmann, F. Reinker, S. Wiesche, E. Y. Kenig and F. V. J. Dubberke, *Performence Predictions of Axial Turbines for Organic Rankine Cycle (ORC) Applications Based on Measurements of the Flow Through Two-Dimensional Cascades of Blades*, in Proceedings of the ASME 2014 Power Conference, POWER2014-32098, Baltimore, USA (2014)
19. K. Gersten, *Fully Developed Turbulent Pipe Flow*, in Fluid Mechanics of Flow Metering, Berlin, Heidelberg, Springer (2005)
20. D. Händel, R. Niehuis and U. Rockstroh, *Aerodynamic Investigations of a Variable Inlet Guide Vane with Symmetric Profile*, in Proceedings of ASME Turbo Expo, GT2014-26900, Düsseldorf, Germany (2014)